

# JOURNAL OF ADVANCED APPLIED SCIENCES

e-ISSN: 2979-9759



#### RESEARCH ARTICLE

# Investigation of the Effect of Electrode Type on Microstructure and Mechanical Properties in the Welding Process of Millux 500 Protection Armour Steels with Shielded Metal Arc Welding Method

Hakan Ada<sup>1,2™</sup> • Muhammed Ahmet Çobanoğlu³ • Nihat Kaya⁴ •

#### ARTICLE INFO

#### **Article History**

Received: 22.10.2024 Accepted: 10.12.2024 First Published: 30.12.2024

#### Keywords

Armour steel Citochromax Miilux Protection 500 Shielded metal arc welding Tenacito 80



#### **ABSTRACT**

This study highlights the critical importance of electrode selection in ensuring the mechanical integrity and metallurgical reliability of welded armour steel, contributing valuable insights for future applications in the defence industry. In this study, plates produced from Miilux Protection 500 armour steel were joined by the electric arc welding method with Citochromax and Tenacito 80 shielded electrodes produced by Magmaweld. To characterise the mechanical and metallurgical performances of the joints, tensile, hardness and bending tests were performed on the samples taken from the joints and optical microscope and SEM examinations were performed. When all the results were evaluated in the shielded electrode electric arc welding applications of Protection 500 armour sheets of steel, the most suitable metallurgical and mechanical performance electrode was Tenacito 80.

#### Please cite this paper as follows:

Ada, H., Çobanoğlu, M. A., & Kaya, N. (2024). Investigation of the effect of electrode type on microstructure and mechanical properties in the welding process of Miilux 500 Protection armour steels with shielded metal arc welding method. *Journal of Advanced Applied Sciences*, 3(2), 55-65. https://doi.org/10.61326/jaasci.v3i2.300

#### 1. Introduction

Throughout history, humanity has instinctively wanted to survive and sustain its life. With this instinctive effect, it has developed itself against various threats from nature. In the early periods, these developments appear as shelters, caves and dwellings for shelter. With the impact of harsh living conditions and harsh conditions, the need for protection has evolved from

structural protection to personal protection. Within the scope of personal protection, people have tried to take precautions against complex natural conditions and threats such as attacks, wild animal attacks, bumps, impacts and various injuries by developing protective clothing, covers, headgear and footwear (Baykara et al., 2020).

E-mail address: hakanada@gazi.edu.tr



<sup>&</sup>lt;sup>1</sup>Gazi University, Faculty of Technology, Department of Metallurgical and Materials Engineering, Ankara/Türkiye

<sup>&</sup>lt;sup>2</sup>Kastamonu University, Faculty of Engineering and Architecture, Department of Mechanical Engineering, Kastamonu/Türkiye

<sup>&</sup>lt;sup>3</sup>Kastamonu University, Institute of Science, Department of Mechanical Engineering, Kastamonu/Türkiye

<sup>&</sup>lt;sup>4</sup>Osmaniye Korkut Ata University, Kadirli Vocational School, Department of Mechanical Program, Osmaniye/Türkiye

<sup>&</sup>lt;sup>™</sup> Correspondence

The materials used for personal protection became unable to fulfil their primary task with the development of threat elements, and this situation forced the development of materials used in personal protection, which are defence materials. The use of threat elements such as spears and axes made with complex and sharp-edged rocks revealed the weakness of defence materials, and with the development of metal production and processing skills, the era of metallic materials as personal protection began. With the discovery of alloying, people saw that bronze was effective in personal protection and attack materials and applied alloying to threat and defence materials. In response to various threats, various personal protective materials have been produced, leading to the concept of armour (Baykara et al., 2020).

While in the past, sharp axes, spears and arrows constituted threat members, today, advanced modern weapons, kinematic

and explosive projectiles, grenades, and mines constitute threat members. Subsequently, the development of armour materials has become a necessity. Modern armour materials include metal, polymer, ceramic and composite-based armour. When the developments are examined, it is seen that threat elements and armour materials that will eliminate threat elements have developed in parallel over time (Kara, 2012).

Armour materials must maintain their structural integrity and resist cracking, fragmentation, and breakage against various kinematic projectiles that will apply impact loads to fulfil and continue their mission against the threat element (Laible, 1980). In this respect, armour materials should be selected by considering the characteristics of threat elements and armour materials. Table 1 below shows the armour materials used against 7.62 and 14.5 mm armour-piercing ammunition.

Table 1. Armour materials used against 7.62 and 14.5 mm armour-piercing bullets (Karagöz & Atapek, 2007).

Armour Materials						
Steel	Glass Reinforced E-cam					
- RHA (380 HB)	- S glass					
- High Hardness (550 HB)						
- Dual Hardness Armour (440-600 HB)						
Aluminum	Ceramic					
- 5083 alloy	- Aluminum oxide					
- 7039 alloy	- Aluminum oxide + Al					
- 2519 alloy	- Boron carbide					
•	- Titanium dicarbide					
Compos	site (Multilayer with ceramic surface)					
_	Al + RHA					
	Steel + RHA					
	E glass + RHA					

Metallic armour has become one of the prominent materials in modern armour technologies thanks to its wide range of mechanical properties and high production speeds, compared to other armour materials that offer different advantages in various application areas. Metallic armours are produced by alloying and heat treatment processes and are armour materials that effectively prevent various threat elements (Laible, 1980). Metallic armours are preferred to achieve desired mechanical properties such as hardness, toughness and strength. Thanks to their excellent formability, ductility and weldability, these armours can be formed to the desired size and shape and provide high production speeds. Metallic armours are generally divided into four main groups: aluminium, magnesium, steel and titanium (Hazell, 2022). Today, aluminium and steel metallic armours are prominent in machinability, cost and weldability to the desired geometry (Hazell, 2022).

Armour steels are one of the most essential materials that form the basis of widely used armour steels. It is constantly being improved metallurgically and mechanically. It is among the most preferred materials due to its superior ballistic performance and high weldability during manufacturing (Baykara et al., 2020). Reinforced steel sheets should be used in armoured vehicles where protection is required. Mechanical properties such as high tensile strength, yield strength and hardness are among the main reasons these steel sheets are preferred. However, the plastic deformation process is complicated in armour steels with high mechanical properties and strength. Cracks along the bend line may occur in the armour steel during deformation.

Since armour steels have high mechanical properties and strength, high forces must be applied during forming. Due to its poor plastic deformation capability, welding is one of the most suitable methods for bringing armour steels to the desired size and geometry. The methods used in welding armour steels include electric arc welding with covered electrodes, gas arc welding (TIG, MIG, MAG) and submerged arc welding. One of the most widely used methods is electric arc welding with a shielded electrode. Although this method is convenient, if the electrode contains moisture, there is a risk of hydrogen penetrating the weld zone and causing cracks during cooling. It is, therefore, important that the electrodes are thoroughly dried and free of moisture. In gas metal arc welding, the risk of

hydrogen is lower as there is no shroud to protect the welding bath. However, electrodes with low hydrogen content should be preferred for gas metal arc wire electrodes. Submerged arc welding can be used for long and linear welding processes. This method enables faster welding of armour steels with significant wall thickness. However, attention should be paid to the powder's hydrogen and moisture content (Yakut, 2015).

In welded joining processes, it is essential to determine the welding method and the filler material that best suits the chemical and mechanical properties of the base material. In a basic welded jointing process, the aim is for the weld seam to have higher mechanical properties than the base material. However, this is not yet possible for armour steels. In welding armour steels subjected to dynamic stress, pressure and impact, and cracking sensitivity, filler materials that exhibit higher mechanical properties than the base material have not yet been developed. For this reason, filler materials with good wetting properties, suitable for filling and forming a stress-relieving buffer layer, are generally preferred. These materials are used in welded joints, even though they are far from providing the mechanical properties of the base material (Gürol et al., 2022).

Miilux Protection 500 armour steel plates were joined in this study using the shielded electrode electric arc welding (SMAW) method. In this process, two different commercially

available electrode wires (Citochromax and Tenacito 80), which were determined to be of suitable composition for the study, were preferred. The study aims to evaluate the effects of these filler materials used in industrial applications and the applied current intensity values on the mechanical and metallurgical properties of Miilux Protection 500 sheets of steel by comparative analysis. These analyses aim to reveal the effects of different electrodes and current intensities on the performance of Miilux Protection 500 steels.

#### 2. Materials and Methods

In this study, armour steels of MIL-A 46100 class, which have high hardness and strength, were welded by arc welding with a shielded electrode. The welding speeds were kept constant, and the effects of changes in current strength on the microstructure and mechanical properties of the welded joints were investigated.

#### 2.1. Material

Miilux Protection 500 armour steel with a section thickness of 4.2 mm and a hardness value of approximately 500 HBW was used in this study. The chemical composition and mechanical properties of Miilux Protection 500 armour steel are presented in Table 2.

**Table 2.** Chemical composition and mechanical properties of the armour steel used.

Steel	Thickness	Element (%)								
Quality	(mm)	С	Si	Mn	P	S	Cr	Ni	Mo	В
	4.00-40.00	0.30	0.70	1.70	0.015	0.005	0.75	0.80	0.50	0.004
Miilux Protection 500	Hardness HBW	$\mathbf{R}_{\mathbf{l}}$	Strength p 0.2 (IPa)	Tensile Rm (I	Strength MPa)	Elong (%	gation o)	Resis	Impact stance C) Joule	Carbon Equivalence (Ceq)
	480-560	1.	300	16	500	8			17	0.70

In this study, two different electrodes were selected for the welded joining of Miilux Protection 500 armour steels. The 3.25 mm diameter electrodes were produced by Magmaweld and named as Citochromax and Tenacito 80. The detailed list

of these materials according to standards and company is presented in Table 3, and their chemical composition and mechanical properties are presented in Table 4.

**Table 3.** Nomenclature of the materials used in the study according to standards and company.

Filler Metal	Magmaweld Code	Standard and Nomenclature	AWS Code and Nomenclature
Diameter (m	nm)		
	Citochromax	TS EN ISO 3581 - A	AWS/ASME SFA - 5.4
3.25 —		E 18 8 Mn B 22	E307-15
3.23	Tenacito 80	TS EN ISO 18275 - A	AWS/ASME SFA - 5.5
		E 69 6 Mn2NiCrMo B 42 H5	E11018-G H4

Table 4. Chemical composition and mechanical properties of the filler wires used in the study.

Eillen Metal Tyme				El	ement (	%)		
Filler Metal Type	C	Si	Mn	Cr	Ni	Mo	S	P
Citochromax	0.12	0.40	6.00	19.00	9.00	-	≤0.020	≤0.025
Tenacito 80	0.06	0.50	1.80	0.35	2.20	0.40	≤0.012	≤0.020

	Mechanical Properties							
Filler Metal Ty	Yield ype Strength (MPa)	Tensile Strength (MPa)	Elongation (%)	Impact Resistance (Joule) and Test Temperature				
Citochromax	480	660	40	70 (20 °C)				
Tenacito 80	775	890	18	50 (-60 °C)				

#### 2.2. Method

Birikim Engineering and Industrial Contracting Inc. carried out the welded joints of Miilux Protection 500 armour steels in Ankara by the standards. The plates prepared for welded joints were cut in 380x200x4.2 mm dimensions by TS EN ISO 15614-1 standard, considering the sample sizes required for test examinations. The beveling process of the supplied plates was carried out according to TS EN ISO 9692-1 standard and taking into account the filler material diameter. Y-type weld bead geometry was used in the study. The schematic representation of the weld bead geometry is given in Figure 1, and the weld bead dimensions determined according to the diameter of the filler metal are given in Table 5.

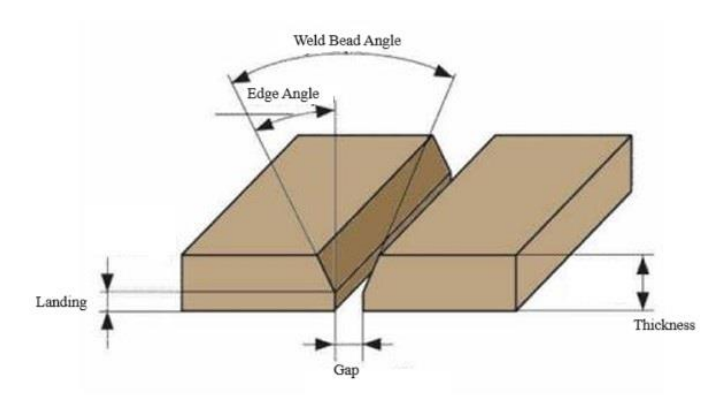


Figure 1. Demonstration of weld bead geometry.

**Table 5.** Measurements of weld bead geometries.

Thickness	Gap	Landing	Weld Bead Angle	Edge Angle
(mm)	(mm)	(mm)	(°)	(°)
4.2	3.5	2.00	50	25

The welding parameters used in the welded joints of Miilux Protection 500 armour steel are presented in Table 6. According

to Table 6, the current intensity values used in the experiments were determined based on the catalogue data of the electrode manufacturers and were selected as 100, 110 and 120 Amperes, respectively. Arc voltage and welding speed were kept constant in the experiments.

This study performed mechanical tests and microstructural investigations for each experiment. Mechanical tests include tensile, bending and hardness tests, which evaluate the mechanical performance of welded joints. Since armour steels are considered to be heat sensitive, the specimens were cut using a water jet. Sanding and polishing the samples for microstructure and macrostructure examinations performed on a Siemens brand device. By the metallographic examination standards, 80, 120, 240, 240, 400, 800, 1200 and 2500 grit abrasives were used, and the samples were polished with 3 and 1 µm diamond solutions, respectively, using polishing felts. In order to determine the resistance of the polished specimens to plastic deformation, hardness tests were performed on the specimens after microstructure examination. Hardness measurements were carried out with 50 measurements from 25 points at equal distances to the weld centre's left (-) and right (+) until the base material's hardness was determined per TS EN ISO 9015-2 standard (Figure 2). The distance between hardness measurements was set as 0.5 mm, and the centre of the weld metal (point 0) was taken as the reference point. Since it was observed that the hardness values of the base material could not be reached due to the HAZ (Heat-Affected Zone) width caused by the heat input effect, additional hardness measurements were made at 1 mm intervals from point 26 to point 37, where the base material hardness values were obtained. Hardness tests were performed using the Shimadzu brand and HMV-G21 model device under 1 kg load and the Vickers hardness measurement method.

Table 6. Welding parameters.

Experiment No.	Electrode	Diameter (mm)	Current Intensity (Ampere)	Voltage (V)	Welding Speed (cm/min)
N1			100		
N2	Citochromax	G2 25	110		0.5
N3			120	22.5	
N4		—— Ø3.25	100	22.5	9.5
N5	Tenacito 80		110		
N6			120		

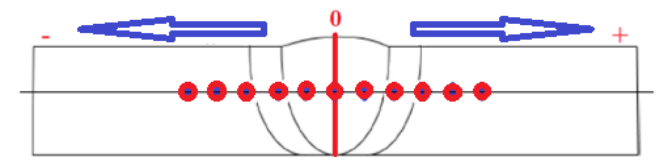


**Figure 2.** Schematic representation of hardness tests.

For tensile tests, specimens taken from welded joint plates were prepared by the TS EN ISO 4136 standard and specimens taken from the base material were prepared by the TS EN ISO 6892-1 standard. Tensile specimens prepared by the standards were tested at room temperature with an Instron brand 8503 model device with 500 kN capacity. In order to measure the elongation of the specimens during the tensile process, the first measurement length was marked on the specimens before the test, and the elongation amounts were determined by measurements made after the test.

In order to evaluate the elastic and plastic deformations of the materials joined by the welding process and to check the suitability of the weld, test specimens were prepared by TS EN ISO 5173 standard and bending tests were performed. Bending tests were performed with a 500 kN capacity Hidroliksan brand device. The tests were performed at room temperature,  $180^{\circ}$  bending angle and using a 20 mm diameter chuck, and the distance between the bearings was set to 28.4 mm.

#### 3. Results

Macrostructure, microstructure, hardness, tensile and bending tests were performed on the samples taken from the welded joints and the findings are presented below.

## 3.1. Macrostructure Review

From the macrostructure images, it is clear that the penetrations are complete, and, as expected, the melting line and HAZ in the weld zone are observed. When the macrostructure images in Figure 3 and Figure 4 are evaluated, the melting line and HAZ are more clearly observed in the macrostructures of the welds made with Citochromax-coded weld metal showing austenitic stainless steel properties and in the images of the joints made with Tenacito 80 welding materials showing ferritic properties. It is observed that the grains are directed towards the weld centre in the direction of heat escape.



Figure 3. Macrostructure images of the welded joint made with the Citochromax coded electrode (Ø3.25 mm) a) N1, b) N2 and c) N3.

Figure 4. Macrostructure images of the welded joint made with Tenacito 80 electrode (Ø3.25 mm) a) N4, b) N5 and c) N6.

#### 3.2. Microstructure Review

In order to evaluate the microstructural effects of Protection 500 welds made at various current values using the shielded electrode arc welding method, optical microscope examinations were performed on the samples. Microstructure images were obtained at 200 and 500 times magnification. The microstructure image of the base material is shown in Figure 5.

The optical microscope images in the figure show that the base material exhibits a fine-grained microstructure. The images show that martensitic and ferritic regions are dominant in the microstructure. While the martensitic structure gives armour steels high hardness and strength, it occurs in needle-like and slat-type forms. In addition, needle-shaped and tapered acicular ferrites exhibit similar hardness effects (Jena et al., 2010).



**Figure 5.** Microstructure images of Miilux Protection 500 base material.

Microstructure images of welded joints are given in Figure 6. Citochromax electrode belongs to the austenitic stainless steel electrode class. This electrode contains approximately 8% Nickel (Ni) by weight, directly affecting the formation of the austenite phase. While the austenitic structure is formed with this electrode, a limited amount of delta ferrite is formed within the austenitic matrix during the joining processes. This creates ferritic structures in the weld metal, especially at the grain boundaries. The Tenacito 80 electrode, with its low carbon content, provides an excellent combination of strength and toughness in welded joints. This electrode forms an acicular ferrite microstructure of ferrite plates nested within austenite grains. Acicular ferrite is the most desirable structure in low-carbon steels and produces fine-grain structures. This allows high mechanical properties to be achieved in welded joints.

#### 4. Discussion

# 4.1. Tensile Test Results

Tensile tests were performed on three specimens of the base material and welded joints. The test results are given in Table 7 and Figure 7. As seen from Table 7, the maximum tensile strengths, the averages of these strengths, % elongation values and % cross-sectional shrinkage of the base material and welded joint specimens were determined as a result of the tensile test. In order to avoid measurement uncertainties, the initial length and cross-sectional area of all specimens were marked before the test, and the post-test elongation and cross-sectional shrinkage were calculated separately.

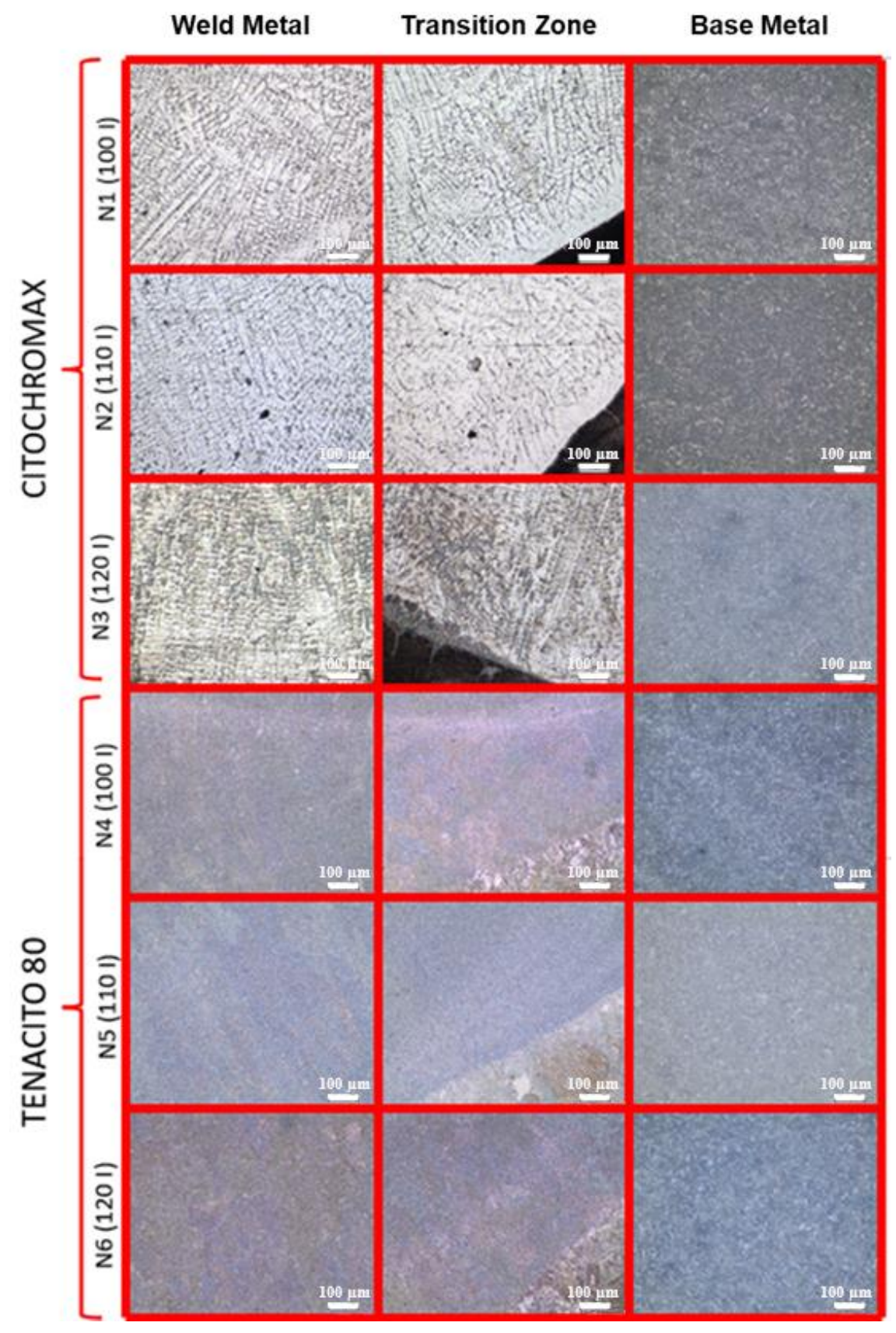


Figure 6. Microstructure images of welded joints.

Table 7. Tensile test results.

Filler Material	Experiment No.	Elongation (%)	Average Tensile Strength (MPa)
Base Mate	erial	6.69	1,768.19
Citochromax	N1	1.96	852.20
chro	N2	1.85	796.77
Cito	N3	2.44	867.85
08	N4	4.30	951.24
Tenacito 80	N5	5.15	957.31
Ten	N6	5.12	940.98

When the tensile test result graph presented in Figure 7 is examined, it is seen that Protection 500 base material has a very high strength value. This material is used as an armour material due to its superior mechanical properties. However, during the welding process, there are significant differences between the strength values of the welded joints and the strength values of the base material due to the lack of a suitable electrode type for the base material and the heat applied negatively affects these superior properties of the armour steel. This is an expected result. Despite these expectations, in this study, suitable filler materials that can be used in welded joint processes for Protection 500 material were determined, and the metallurgical and mechanical performances of these materials were examined. In this way, it aims to create a guiding study for users regarding industrial use.

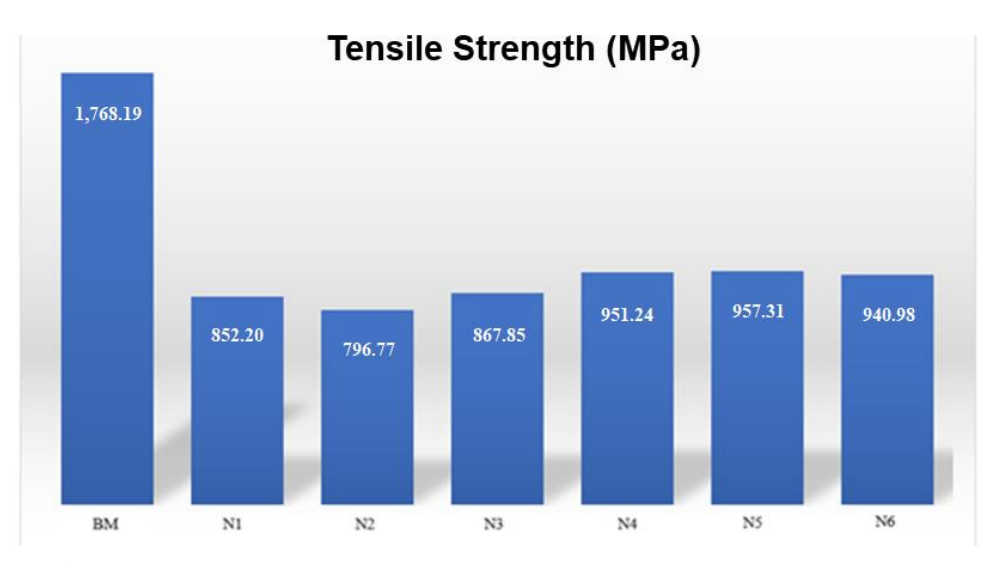


Figure 7. Tensile test results.

The maximum tensile strength of the welded joints was compared with the maximum tensile strength of the base material. The tensile test applied to the samples taken from the base material resulted in an average tensile strength of 1,768.19 MPa. The highest maximum tensile strength was obtained in experiment N5 with an average of 957.31 MPa with a Tenacito 80 coded electrode, and the lowest maximum tensile strength was obtained in experiment N2 with an average of 796.77 MPa with a Citochromax coded electrode. In all welded joints, ruptures occurred from the centre of the weld metal.

#### 4.2. Hardness Investigations

Hardness tests were conducted on welded plates to measure the resistance of welded joints against plastic deformation. In this study, 75 measurements were taken from each welded sample. The hardness results of the welded joints made using shielded electrodes are shown in Figure 8. To minimise measurement uncertainties, all results are presented within a tolerance range of  $\pm 5~{\rm HV}.$ 

When examining the hardness test result graphs, it was observed that similar hardness curves were formed in all joints. The hardness graphs obtained from the welded joints with different parameters on Protection 500 material generally resemble each other. However, the hardness values vary depending on the current intensity and electrode type. In all experiments' hardness graphs, the region with the highest hardness is the HAZ, while the region with the lowest hardness is the weld metal zone. This situation is similar to other studies on weldability (Aksöz et al., 2017a; Çetinkaya et al., 2023).

It has been observed that the heat applied during the welding processes creates a heat treatment effect on the material, affecting specific areas. The experiments revealed that the highest hardness values were obtained in the HAZ. In experiments with high current intensity, the amount of heat entering the material increased, resulting in coarser grains and a wider spread of the HAZ. According to the data obtained from tensile tests, it was observed that the HAZ expanded in experiments with higher heat application and larger grains

formed. This situation led to a decrease in the strength values of the joints while causing an increase in the percentage elongation values. In experiments where coarse-grained structures were formed, lower hardness values were measured compared to other experiments that resulted in finer-grained structures due to the effects of applied current intensity and

cooling rate. The values obtained from the tensile tests confirmed the directly proportional relationship between hardness and strength. This situation is similar to other studies on weldability (Aksöz et al., 2017b; Çoban et al., 2023; Harman et al., 2022).

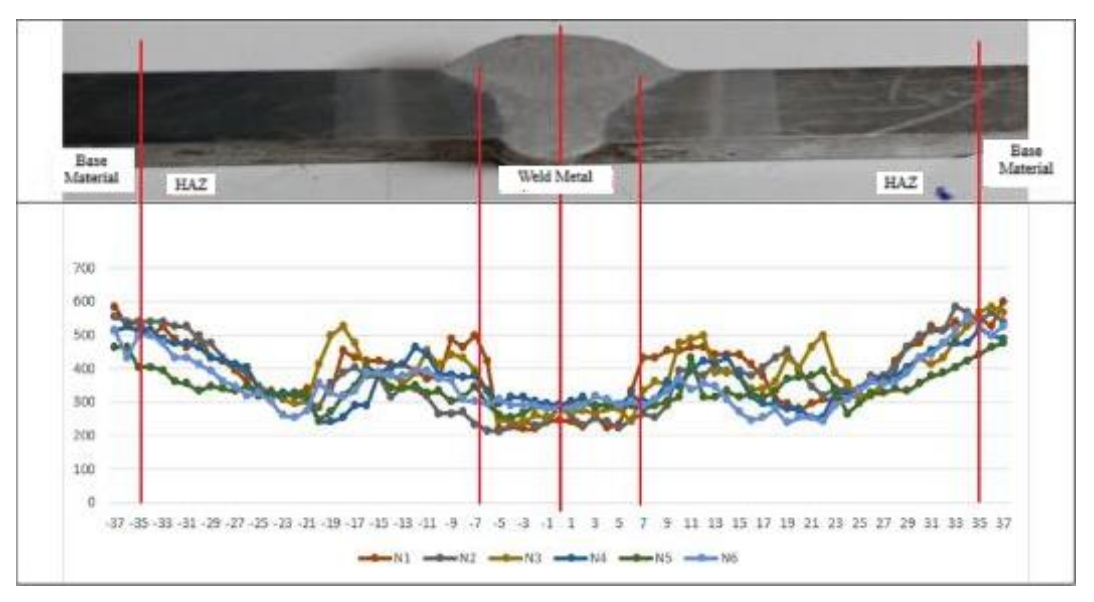


Figure 8. Hardness test results.

### 4.3. Bending Test Results

Bending tests were conducted on samples with the weld region centred by the TS EN ISO 5173 standard. The welded joints were tested in two directions: cap and root bending. 12 bending test samples were prepared, with two samples for each test. These tests aimed to determine whether the welded joints

exhibited a performance close to the ductility of the base material. Additionally, this method revealed potential defects in the welded joints, confirming their suitability. The acceptable welded joints reached a bending angle of  $180^{\circ}$ , while the unsuitable ones are presented in Table 8 with their fracture angles within a tolerance range of  $\pm 2^{\circ}$ .

**Table 8.** Bending test results.

Filler Metal	Experiment No.	Current Intensity	Filler Metal Diameter (mm)	Mandrel Diameter (mm)	Support Span (mm)	Bending Angle (°)	Face Bend Angle (°)	Root Bend Angle (°)
nax	N1	100					180°	175°
Citochromax	N2	110		20	28.4	180	72°	65°
Citc	N3	120	_ 3.25				54°	175°
80	N4	100	3.23				180°	74°
Tenacito 80	N5	110					180°	180°
Ter	N6	120					180°	55°

As a result of the bending tests, the samples that underwent plastic deformation are shown in Figures 9 and 10. In order to avoid repetition in the visualisation, images of the bent specimens obtained from experiments carried out with an average current intensity of 110 A for each type of electrode are shown. During the bending test, the samples were subjected to compressive stresses on the inner surfaces and tensile stresses on the outer surfaces. As a result, expansion occurred on the

inner surface, while cross-sectional reductions occurred on the outer surface.



Figure 9. Bended specimens.



Figure 10. Bended specimens.

#### 5. Conclusion

In this study, Miilux Protection 500 armour steels were welded using shielded metal arc welding with Citochromax and Tenacito 80 electrodes, and the microstructure and mechanical properties of the welded joints were examined. The results obtained from the study are summarised below.

- From the macrostructure images, it can be seen that the penetrations have formed completely and as expected; the fusion line and HAZ in the weld region are observed.
- Microstructural investigations revealed the formation of austenitic and ferritic microstructures, while it was determined that martensitic and acicular ferrite structures predominated in the weld metal.
- The tensile tests showed that the Protection 500 base material has a significantly high strength value. The highest maximum tensile strength in the welded joints was obtained in the N5 experiment using the TENACITO 80 electrode, averaging 957.31 MPa. In contrast, the lowest maximum tensile strength was recorded in the N2 experiment welded with the CITOCHROMAX electrode, averaging 796.77 MPa.
- In the tensile tests, the fractures in the welded joints occurred as expected from the weld metal.

- In the hardness graphs obtained from welded joints made with different parameters on Protection 500 material, the hardness values varied according to the applied current intensity and electrode type.
- In the hardness graphs of all experiments, the region with the highest hardness was measured as the HAZ, while the region with the lowest hardness was the weld metal zone.

# Acknowledgment

This manuscript study was presented as an abstract at the 5<sup>th</sup> International Congress on Engineering and Life Science held in Romania on September 10-12, 2024. In addition, the authors would like to thank Kastamonu University Scientific Research Projects Coordinatorship for supporting the study with the project number KÜ-BAP01/2019-34, Birikim Engineering Company where the welded joints were made, Magmaweld where filler materials were supplied, Kastamonu University Faculty of Engineering and Architecture, Department of Mechanical Engineering where microstructure and hardness examinations were performed, Gazi University Faculty of Technology, Department of Metallurgical and Materials Engineering where tensile tests were performed, Karabük University Faculty of Technology, and Department of Manufacturing Engineering where macro images were taken and bending tests were performed.

#### **Conflict of Interest**

The authors declare that they have no conflict of interest.

#### References

Aksöz, S., Ada, H., & Özer, A. (2017a). Toz altı kaynak yöntemiyle üretilen API 51 x70 kalite çelik boruların mikroyapı ve mekanik özellikleri. *Gazi Üniversitesi Fen Bilimleri Dergisi Part C: Tasarım ve Teknoloji*, 5(1), 55-64. (In Turkish)

Aksöz, S., Ada, H., Fındık, T., Çetinkaya, C., Bostan, B., & Candan, İ. (2017b). API 5L X65 çeliklerinin elektrik ark kaynak yöntemi ile birleştirilmesinde, kaynak işleminin mikroyapı ve mekanik özelliklere etkisinin incelenmesi. *El-Cezerî*, 4(1), 72-81. <a href="https://doi.org/10.31202/ecjse.289639">https://doi.org/10.31202/ecjse.289639</a> (In Turkish)

Baykara, T., Günay, V., & Demirural, V. (2020). *Zırh teknolojileri*. Yeditepe Ünivesitesi Yayınevi. (In Turkish)

Çetinkaya, C., Taşçı, S., & Ada, H. (2023). 3Cr12 ferritik paslanmaz çeliklerin gaz metal ark kaynağıyla birleştirilmesinde ilave tel türünün mikroyapı ve mekanik özelliklere etkisinin araştırılması. *Politeknik Dergisi*, 26(4), 1651-1660. <a href="https://doi.org/10.2339/politeknik.1392366">https://doi.org/10.2339/politeknik.1392366</a> (In Turkish)

Çoban, M., Ada, H., & Çetinkaya, C. (2023). AISI 304l östenitik paslanmaz çeliklerin lazer kaynağıyla birleştirilmesinde nitrasyon işleminin mikroyapı ve

- mekanik özelliklere etkisinin araştırılması. *Gazi Üniversitesi Fen Bilimleri Dergisi Part C: Tasarım ve Teknoloji*, *11*(4), 1171-1182. https://doi.org/10.29109/gujsc.1388280 (In Turkish)
- Gürol, U., Karahan, T., Erdöl, S., Çoban, O., Baykal, H., & Koçak, M. (2022). Characterization of armour steel welds using austenitic and ferritic filler metals. *Transactions of the Indian Institute of Metals*, 75, 757-770. https://doi.org/10.1007/s12666-021-02464-7
- Harman, M., Ada, H., & Çetinkaya, C. (2022). QStE420TM çelik malzemelerin farklı bazik elektrodlar kullanılarak örtülü elektrodla ark kaynak yöntemiyle kaynaklanabilirliğinin araştırılması. *Gazi Üniversitesi Mühendislik Mimarlık Fakültesi Dergisi*, *37*(4), 2041-2056. <a href="https://doi.org/10.17341/gazimmfd.893705">https://doi.org/10.17341/gazimmfd.893705</a> (In Turkish)
- Hazell, P. J. (2022). *Armour: Materials, theory, and design*. CRC Press. <a href="https://doi.org/10.1201/9781003322719">https://doi.org/10.1201/9781003322719</a>

- Jena, P. K., Mishra, B., RameshBabu, M., Babu, A., Singh, A. K., SivaKumar, K., & Bhat, T. B. (2010). Effect of heat treatment on mechanical and ballistic properties of a high strength armour steel. *International Journal of Impact Engineering*, 37(3), 242-249. <a href="https://doi.org/10.1016/j.ijimpeng.2009.09.003">https://doi.org/10.1016/j.ijimpeng.2009.09.003</a>
- Kara, S. (2012). Çelik esaslı zırh malzemesinin 307si elektrodu ile kaynak edilebilirliğinin ve mikroyapı üzerindeki etkisinin deneysel araştırılması (Master's thesis, Fırat University). (İn Turkish)
- Karagöz, Ş., & Atapek, H. (2007). *Bor katkılı zırh çeliklerinin kırılma davranışı*. 8. Uluslar Arası Kırılma Konferansı. İstanbul. (In Turkish)
- Laible, R. C. (1980). *Ballistic materials and penetration mechanics*. Elsevier Scientific Publishing.
- Yakut, V. (2015). Zırh çeliklerinin ferritik ve östenitik dolgu malzemeleriyle kaynağının incelenmesi (Master's thesis, Sakarya University). (In Turkish)